Chemical Physics Letters 560 (2013) 55–59

Contents lists available at SciVerse ScienceDirect

Chemical Physics Letters

journal homepage: www.elsevier.com/locate/cplett

Terahertz time-domain and FTIR spectroscopic study of interaction of α-chymotrypsin and protonated tris with 18-crown-6

A.A. Mankova [a,*], A.V. Borodin [a], A.V. Kargovsky [a], N.N. Brandt [a], Q. Luo [b], I.K. Sakodynskaya [c], K. Wang [b], H. Zhao [b], A.Yu. Chikishev [a], A.P. Shkurinov [a], X.-C. Zhang [d]

[a] Department of Physics and International Laser Center, M.V. Lomonosov Moscow State University, Moscow 119992, Russia
[b] Wuhan National Laboratory for Optoelectronics, Huazhong University of Science and Technology (HUST), 1037 Luoyu Road, Wuhan 430074, PR China
[c] Department of Chemistry, M.V. Lomonosov Moscow State University, Moscow 119992, Russia
[d] The Institute of Optics, University of Rochester, 275 Hutchison Rd., 114 Wilmot Building, Rochester, NY 14627-0186, USA

ARTICLE INFO

Article history:
Received 21 November 2012
In final form 28 December 2012
Available online 12 January 2013

ABSTRACT

Chymotrypsin activity in nonaqueous solvents increases in the presence of crown-ethers, presumably, due to the interaction of crown-ether molecules with surface amino-groups of protein. FTIR and THz-TDS spectroscopic techniques are used to study the interaction of crown-ether with chymotrypsin and protonated tris(hydroxymethyl)aminomethane, which serves as a model of the amino-groups of protein. Spectra measured at different relative molar concentrations indicate the interaction of the components. The spectral changes and variations in the absolute values of the absorption coefficient are discussed. The similarity of the spectral changes is demonstrated for protein-crown–ether and tris-crown–ether samples.

1. Introduction

The analysis of biological molecules is among central problems in physics, chemistry and biology. Enzymes are important biological molecules that control functioning of living organisms. Enzymatic activity is normally related to their conformational dynamics, so that the structural features of enzymes play an important role in functioning.

Water is natural environment for a significant part of enzymes. When the environment is modified, the free energy of protein globule changes and a new equilibrium is reached due to variations in spatial structure. The analysis of the function-related structural modifications of enzymes in various media is necessary when the control of enzymatic activity is considered.

In water, serine proteases provide the hydrolysis of peptide bonds and, for example, for α-chymotrypsin (CT), the maximum activity is reached at pH 7.8 [1]. When the lyophilized proteases are placed in organic solvents, the functioning changes to transesterification and the activity decreases by a few orders of magnitude [2,3]. However, the activity in organic solvents substantially increases if the serine protease is lyophilized from the aqueous solution containing crown ether. The maximum activities are different in different solvents and are reached at different relative molar concentrations of enzyme and crown ether (e.g., 1:250 and 1:50 for CT in cyclohexane and acetonitrile, respectively) [4,5]. One of the possible reasons for such an increase in the enzymatic activity is the interaction of crown ether molecules with the surface amino groups of protein [6–11]. To simulate such interaction in this work, we employ a chemical model based on tris(hydroxymethyl)aminomethane (tris). It was demonstrated [12,13] that unprotonated tris weakly interacted with crown ether whereas a relatively stable complex was possible for the tris with protonated amino group (protonated tris).

The methods of vibrational spectroscopy allow the study of the structure and conformation of functional groups. In this Letter, we use terahertz time-domain (THz-TDS) and FTIR spectroscopic techniques in the study of the interaction of CT (serine protease) and protonated tris with 18-crown-6 (CE). Both spectroscopic methods make it possible to study low-frequency vibrational modes. The spectral features can be assigned to the collective motions that consist of both intra- and intermolecular oscillations in a unit cell of molecular crystal [14]. In both cases, line shapes and intensities strongly depend also on the microenvironment of the molecule under study [15].

2. Experimental

2.1. Samples

In the experiments, we used tris and CE from Reakhim and CT from Samson Med.

The tris-CE mixtures are lyophilized from aqueous solutions at several relative molar concentrations. First, tris is dissolved in

* Corresponding author. Tel.: +8 10 7 499 939 11 06.
E-mail address: mankova@physics.msu.ru (A.A. Mankova).

0009-2614/$ - see front matter © 2013 Elsevier B.V. All rights reserved.
http://dx.doi.org/10.1016/j.cplett.2012.12.050

bidistilled water at a concentration of 60 mg/ml and pH 3 is reached using hydrochloric acid. The solution predominantly contains the protonated tris, since pK_{tris} = 8.06. Then, CE is added to the solution and the resulting tris-to-CE relative molar concentrations are 1:1, 1:2, 1:5, and 1:10. The relative concentration of CE in the samples increases, since the maximum enzymatic activity in non-aqueous solvents is reached when the number of the CE molecules per one protein molecule is noticeably greater than the number of the alleged binding sites of the protein molecule (see below). The 20-h-long lyophilization yields powders consisting of microcrystals with sizes of 40–100 μm.

For THz-TDS measurements, the powders are pressed in tablets with a diameter of 13 mm at a monometer pressure of no less than 20 P using a Specac Atlas Manual 15T hydraulic press.

In the FTIR measurements, relatively high absorption coefficients of the samples under study necessitate a decrease in the thickness of tablets to several tens of microns. Such thin tablets are mechanically unstable and, for the FTIR experiments, we pressed the powders on Parafilm M (laboratory film) circles with a thickness of 120 μm and a diameter of 8 mm.

Similar procedures are used to fabricate chymotrypsin-CE tablets at relative molar concentrations of 1:100 and 1:250. The mixtures are lyophilized from bidistilled water.

2.2. FTIR spectrometer

For the FTIR measurements in the transmission configuration, we used a Nicolet 6700 (Thermo Electron Corporation) spectrometer [16]. The measurements are performed in the spectral interval 50–600 cm^{-1} with a spectral resolution of 2 cm^{-1}.

In the spectral range under study, the Parafilm has relatively low background absorbance (no greater than 0.06) and does not exhibit spectral features. However, the nonuniformity of the distribution of the lyophilized powder over the Parafilm film leads to the optical nonuniformity of the pressed tablet and, hence, gives rise to the scattering of the IR radiation. The shape of the spectrum of the sample pressed on the Parafilm film appears to be identical to the shape of the spectrum of the pressed tablet (when such measurements are possible). However, the absolute optical densities (absorption coefficients) at the main absorption peaks may differ by 10–30% due to slight attenuation of the spectrum in general and the presence of additional background in the spectrum of the sample pressed on the Parafilm film. Thus, the absorption intensities in arbitrary units are plotted on the vertical axes of the FTIR spectra and only relative variations in the spectral intensities and modifications of the spectral shapes are discussed. The FTIR spectra are not smoothed.

2.3. The broadband terahertz-time domain spectroscopy (THz-TDS) apparatus

Several experimental techniques including photoconductive antennas, optical rectification and electro optical sampling are widely used for the generation and detection of THz-TDS pulses [17]. These techniques have disadvantage related to a very narrow spectrum of the terahertz pulses. In this work, we employ an alternative approach based on the light-induced breakdown of gases using high-intensity femtosecond pulses [18,19] and the air biased coherent detection (ABCD) [20,21].

In the experiments, we use a ZOmega ZAP-ABCD THz-TDS spectrometer equipped with a Newport-Spectra Physics MAI-TAI femtosecond laser with a pulse duration of 40 fs, a repetition rate of 1 kHz, and a central wavelength of 800 nm. The THz radiation in the frequency interval 0.1–10 THz can be generated. The spectrometer is based on the THz emission resulting from the photo-ionization of gases with two-color (ω and 2ω) laser field. The setup is placed in a chamber that is purged with molecular nitrogen, so that the THz absorption of water vapor is eliminated. The THz radiation is focused on the sample to a spot with a diameter of about 1 mm.

2.4. THz-TDS data processing and fitting procedures

After measuring the temporal profiles with and without sample the absorption coefficient of the sample is roughly calculated as

$$\alpha(\omega) = -2/d \ln |E_{sample}(\omega)/E_{ref})\omega)|,$$

where $E_{sample}(\omega)$ is the amplitude spectrum of temporal profile with sample and $E_{ref}(\omega)$ is the spectrum of temporal profile without sample. The THz spectra are processed using the computer codes from [22]. Note that the signal-to-noise ratio is relatively low and the Savitzky–Golay smoothing procedure with a 30-points smoothing window was used (the total number of points in each THz spectrum is about 200).

2.5. Computational method

Numerical simulations of vibrational spectra for protonated and unprotonated tris and CE crystals were performed in density functional theory framework using the DMol^3 5.5 quantum-chemical package [23,24]. Perdew–Burke–Ernzerhof (PBE) gradient corrected exchange-correlation functional [25] and DNP (double-numerical with d and p polarization) basis set which is comparable to a 6–31G(d,p) Gaussian-type basis set were used.

Geometry optimization was carried out with following criteria: energy convergence of 10^{-6} Ha, max energy gradient of 10^{-3} Ha Å^{-1}, max displacement of 5 times 10^{-3} Å, threshold for density convergence during the SCF minimization of 10^{-6}, k-point separation of 0.04 Å^{-1}.

Long-range interactions were taken into account using Tkatchenko–Scheffler dispersion correction scheme [26]. Coordinates of atoms within the unit cell were optimized within fixed cell parameters specified by the X-ray diffraction studies of protonated tris [27] and CE [28]. Normal-mode analysis was performed in the harmonic approximation.

The calculations were performed using the SKIF MSU Chebyshev and Lomonosov supercomputers of Moscow State University.

3. Results and discussion

In general, the THz-TDS spectral profiles are similar to the FTIR spectral profiles. As was mentioned, the THz-TDS experiments can be performed in the absence of the Parafilm film, so that the absolute absorption coefficients can be determined.

Fig. 1 demonstrates the THz-TDS and FTIR spectra of the protonated tris and the tris-CE mixtures. The CE spectrum (Figs. 1(f) and (f')) exhibits the bands peaked at 2.0, 3.2, 4.3, 4.7, 5.6, 6.8, and 8.0 THz (75, 108, 143, 169, 190, 228, and 266 cm^{-1}). The vertical bars in Figs. 1(a') and (f') show the calculated frequencies, which are roughly in agreement with the experimental data. The spectrum of tris (Figs. 1(a) and (a')) exhibit the bands peaked at 3.0, 4.1, 5.6, 7.2, and 8.1 THz (100, 138, 186, 240, and 275 cm^{-1}).

Relatively strong interaction with the possible formation of a stable complex for the 1:1 sample, which was demonstrated in [6–11] also follows from Fig. 1(b) and (b'). The spectra of the 1:1 complex crucially differ from the spectra of pure substances and cannot be represented as linear combinations of the spectra of components. Note also that the absolute values of the absorption coefficient of the 1:1 sample are not additive with respect to absorption coefficients of the components (Fig. 1(b) and (b')). We assume that the bands of tris peaked at 3.0 and 4.1 THz are broadened and red-shifted and the background absorption increases in

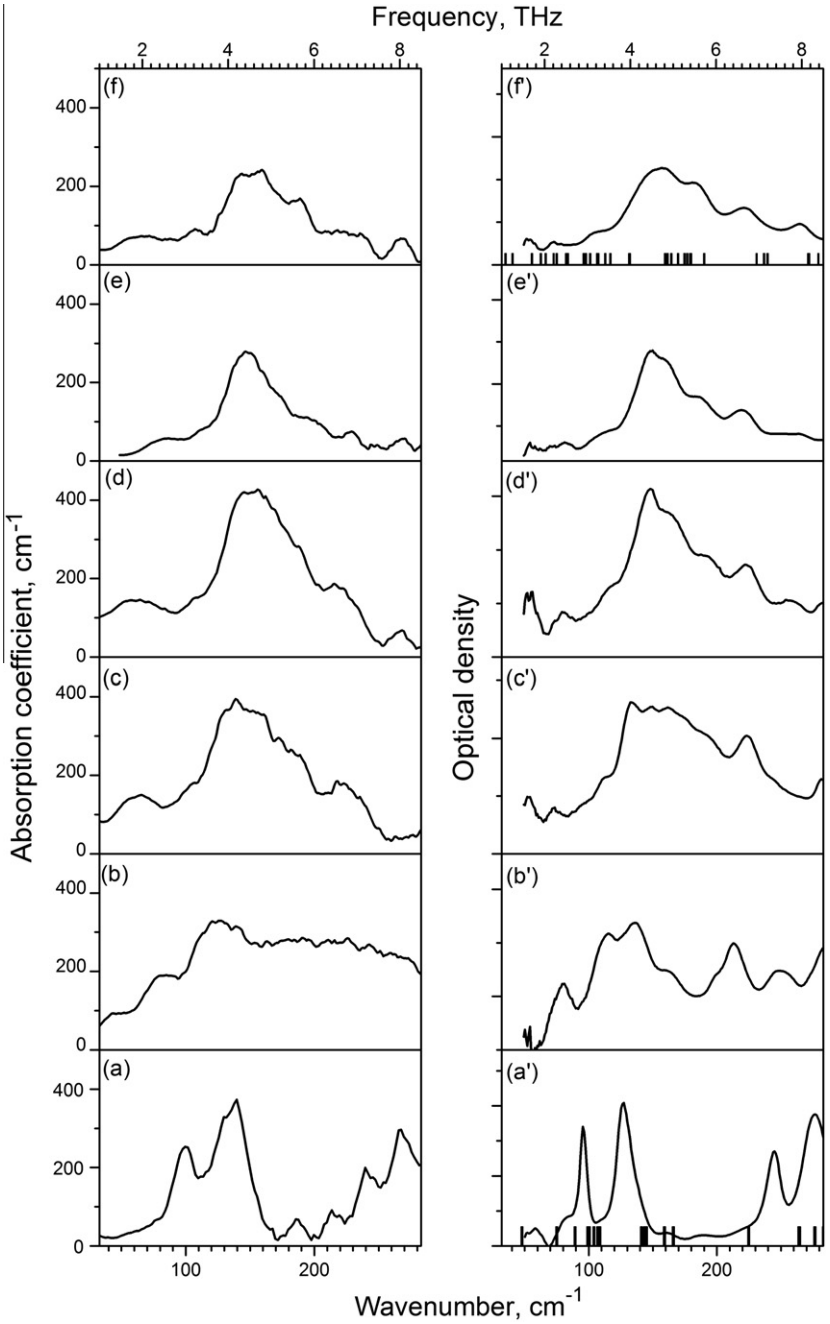

Figure 1. (a) – (f) THz-TDS and (a') – (f') FTIR spectra of (a) and (a') tris; (b) and (b') 1:1, (c) and (c') 1:2, (d) and (d') 1:5, and (e) and (e') 1:10 tris-CE samples; and (f) and (f') CE. The bars in panels (a') and (f') demonstrate the calculated frequencies.

the high-frequency part of the spectrum. Several bands from the spectrum of the 1:1 sample (3.4, 4.1, 6.4, and 7.5 THz (115, 135, 214, and 249 cm^{-1})) are not observed in the CE and tris spectra.

The spectra of the nonequimolar samples (1:2, 1:5, and 1:10) cannot be represented as the sums of the spectra of equimolar sample and CE with the corresponding coefficients depending on the relative concentrations. The spectra of the nonequimolar samples are virtually free of the bands of pure tris, but an increase in the relative concentration of CE gives rise to the bands of CE (3.2, 4.5, 5.6, and 6.8 THz (108, 150, 190, and 228 cm^{-1}). The maximum absorbance of the 1:2 sample (about 400 cm^{-1}) is significantly greater than the maximum absorbances of CE (about 240 cm^{-1}) and equimolar sample (about 330 cm^{-1}). The maximum absorbance of the 1:5 sample is even higher (about 430 cm^{-1}). The spectrum of the 1:2 sample is free of the developed band of the equimolar sample peaked at 250 cm^{-1}.

Thus, the spectra of the samples are gradually modified with an increase in the relative concentration of CE. The bands that are peaked at 3.4 and 4.1 THz (115 and 135 cm^{-1}) in the spectrum of the equimolar sample gradually decrease with an increase in the CE content. The band that is peaked at 193 cm^{-1} in the spectrum of the 1:5 sample is shifted to 186 cm^{-1} in the spectrum of the 1:10 sample and to 182 cm^{-1} in the spectrum of CE. We conclude that the spectra of the tris-CE samples cannot be represented as superpositions of the spectra of components.

Based on the above results, we assume that the tris-CE samples represent at least partially ordered structures with cooperative vibrational modes. A hypothetical unit cell of the 1:2 (1:5) sample

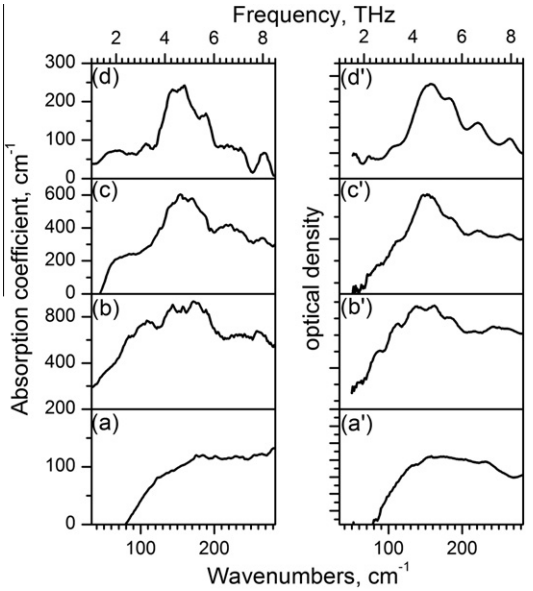

Figure 2. (a) – (d) THz-TDS and (a') – (d') FTIR spectra of (a) and (a') CT; (b) and (b') 1:100, (c) and (c') 1:250 CT-CE samples; and (d) and (d') CE.

may contain 1/3 (1/5) of tris molecules and 2/3 (5/6) of CE molecules. Even when the relative molar concentration of CE is significantly greater than the relative molar concentration of tris, the spectrum of the mixture may differ from the spectrum of pure CE. By way of analogy, the effective scattering potential in the diffraction theory is substantially modified when a single defect is introduced in the periodic atomic chain [29].

Fig. 2 shows the THz-TDS (panels (a)–(d)) and FTIR (panels (a')–(d')) spectra of CT and CT-CE samples. As in the above experiments, the spectral data obtained using the THz spectroscopy are in agreement with the FTIR results. General modifications of the spectra with an increase in the relative concentration of CE are similar to the spectral modifications of the tris-CE samples. Evidently, the minimum number of the possible binding sites on the protein surface is equal to the number of protonated surface amino groups of protein. Note also the possibility of binding with the surface OH groups [7,8]. The number of the binding sites can be estimated using the X-ray data from [30]. At pH < 8, the number of the protonated surface amino groups of CT is no greater than 20. Formal estimation of the surface area of the protein molecule allows about 50 CE molecules to be placed on the surface. Thus, the samples under study contain excess amounts of CE molecules with respect to the number of the possible binding sites on the protein surface.

The CT spectrum represents a relatively smooth curve with weakly developed spectral features peaked at 131, 154, and 234 cm^{-1}. The spectrum of the 1:100 sample substantially differs from the spectrum of protein, and the spectrum of the 1:250 sample differs from the spectrum of protein and appears to be generally similar to the spectrum of CE. Note significantly different maximum absorption coefficients and nonmonotonic variations in the absorbance with a decrease (increase) in the relative concentrations of components.

The general similarity of the spectral shapes in panels (a), (a') and (b), (b') and the presence of the spectral features from the CE spectrum in the spectra of the 1:100 and 1:250 samples makes it possible to assume that the spectra of the CT-CE samples can be represented as superpositions of the spectra of pure substances. Under such an assumption, we can calculate the spectra of the CT-CE samples using the measured spectra of the pure substances (CT and CE) and the relative concentrations of components. We calculate the optical densities of the 1:100 and 1:250 samples assuming the absence of interaction of components (additivity of optical densities) with allowance for the mass ratios of the components (28 wt.% of protein and 72 wt.% of CE in the 1:250 sample and 49 wt.% of protein and 51 wt.% of CE in the 1:100 sample).

Fig. 3 shows that the spectra of the 1:100 and 1:250 samples (solid lines) cannot be represented as linear combinations of the spectra of components with the weighting coefficients determined by the relative concentrations (dashed lines). The comparison makes it possible to assume the interaction of protein and CE, which possibly leads to CE binding. An alternative interpretation may involve the formation of heterogeneous substance in which the CT molecules are embedded in the matrix of CE molecules or vice versa. The 1:100 solid sample can be considered as a lattice of closely packed CT molecules in which the free space between the protein molecules is filled with the CE molecules. Then, in the 1:250 sample, the distance between the protein molecules can be greater than the mean diameter of protein globule by approximately 20%.

Assume that the difference of the spectra of the 1:100 and 1:250 samples is only due to additional amount of CE in the last sample. In other words, assume that the 1:250 sample is an additive mixture of the 1:100 sample and CE. Then, the spectrum of the 1:250 sample must be identical to the linear combination of the spectrum of the 1:100 sample and the spectrum of CE with the corresponding weighting coefficients (we assume the absence of free protein molecules, so that the concentration of the 1:100 species in the 1:250 sample is identical to the concentration of protein). Fig. 4 compares the measured and calculated spectra. It is seen that the spectral shapes are different and the calculated optical density is generally lower than the experimental optical density. Thus, the

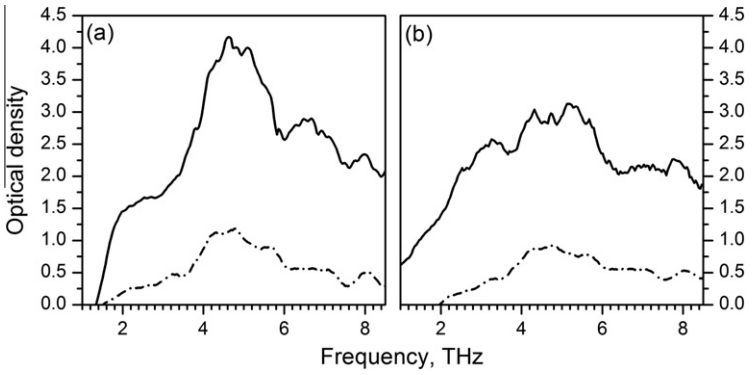

Figure 3. (Solid lines) THz-TDS spectra of (a) 1:250 and (b) 1:100 CT-CE samples and (dashed-and-dotted lines) calculated spectra (see text for details).

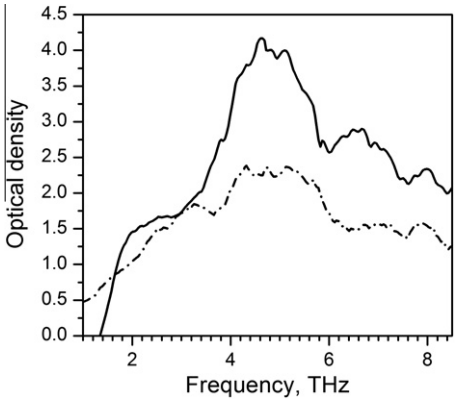

Figure 4. (Solid line) THz-TDS spectrum of 1:250 CT-CE sample and (dashed-and-dotted line) calculated spectrum (see text for details).

additional CE molecules in the 1:250 sample must be at least partially involved in the interaction with the protein molecule and/or cause transformation of the heterogeneous CT-CE system.

4. Conclusions

The absorption spectra of protonated tris, CT, and tris-CE and CT-CE mixtures are measured with the use of THz-TDS and FTIR spectroscopies.

We demonstrate that the protonated tris actively interacts with CE. Apparently, the structures that are formed at different relative molar concentrations of components exhibit spectral features that are absent in the spectra of pure substances.

The CT spectrum demonstrates the broadband absorption with only three weak spectral lines centered at 131, 154, and 234 cm^{-1}. The spectra of the CT-CE mixtures show several developed spectral features. The spectra of the mixtures significantly differ from the spectra of components. The estimations show that the spectra of the 1:100 and 1:250 CT-CE samples cannot be represented as superpositions of the spectra of components and the spectrum of the 1:250 sample cannot be represented as the superposition of the spectrum of the 1:100 sample and the spectrum of CE.

The changes in the spectra of the CT-CE mixtures with an increase in the relative molar concentration of CE are similar to the corresponding changes in the spectra of the tris-CE samples. Thus, we assume that an increase in the functional activity of CT in non-aqueous solvents is related to the interaction of the protonated amino groups of the protein with the CE molecules.

Acknowledgment

The authors gratefully acknowledge partial financial support for this work from the grant of the President of the Russian Federation – NSh-6897.2012.2, Wuhan National Laboratory for Optoelectronics, Huazhong University of Science and Technology (HUST), China and the Russian Foundation for Basic Research (RFBR) (grants 11-02-12248, 11-02-01470 and 12-02-31894-mol_a).

References

[1] A. Fersht, Structure and Mechanism in Protein Science: A Guide to Enzyme Catalysis and Protein Folding, W.H Freeman, 1998.
[2] Y.L. Khmelnitsky, S.H. Welch, D.S. Clark, J.S. Dordick, J. Amer. Chem. Soc. 116 (1994) 2647.
[3] K. Dabulis, A.M. Klibanov, Biotechnol. Bioeng. 41 (1993) 566.
[4] J. Broos, I.K. Sakodinskaya, J.F.J. Engberson, W. Verboom, D.N. Reinhoudt, J. Chem, Chem. Commun. 2 (1995) 255.
[5] D.J. Van Unen, J.F.J. Engberson, D.N. Reinhoudt, Biotechnol. Bioeng. 59 (1998) 553.
[6] N.N. Brandt, V.V. Molodozhenya, I.K. Sakodinskaya, A.Yu. Chikishev, Russian J. Phys. Chem. 74 (11) (2000) 1883.
[7] N.N. Brandt, I.K. Sakodinskaya, A.Yu. Chikishev, Dokl. Akad. Nauk 375 (3) (2000) 1.
[8] N.N. Brandt, I.K. Sakodinskaya, A.Yu. Chikishev, Zh. Fiz, Khim 75 (6) (2001) 1033.
[9] N.N. Brandt, A.Yu. Chikishev, I.K. Sakodinskaya, J. Molecul. Struct. 648 (3) (2003) 177.
[10] H. Tsukube, T. Yamada, S. Shinoda, J. Heterocycl. Chem. 38 (2001) 1401.
[11] J.F.J. Engberson, J. Broos, W. Verboom, D.N. Reinhoudt, Pure Appl. Chem. 68 (1996) 2171.
[12] N.N. Brandt, A.Yu. Chikishev, A.A. Mankova, M.M. Nazarov, I.K. Sakodynskaya, A.P. Shkurinov, Internat. J. 27 (5–6) (2012) 429.
[13] A.A. Mankova, A.V. Borodin, A.V. Kargovsky, N.N. Brandt, I.I. Kuritsyn, Q. Luo, I.K. Sakodynskaya, K.J. Wang, H. Zhao, A.Yu. Chikishev, A.P. Shkurinov, X.-C. Zhang, Chemical Physics Letters 554 (2012) 201.
[14] A.V. Borodin, V. Ya, Opt. Spectrosc. 107 (4) (2009) 505.
[15] R.J. Falconer, A.G. Markelz, J. Infrared Milli Terahertz Waves 33 (2012) 973.
[16] <http://www.thermoscientific.com>.
[17] X.-C. Zhang, J. Xu, Introduction to THz Wave Photonics, Springer Science+Business Media, 2010.
[18] J. Dai, N. Karpowicz, X.-C. Zhang, Phys. Rev. Lett. 103 (2009) 23001.
[19] A.V. Balakin, A.V. Borodin, I.A. Kotelnikov, A.P. Shkurinov, JOSA B 27 (1) (2010) 16.
[20] J. Dai, X. Xie, X.-C. Zhang, Phys. Rev. Lett. 97 (2006) 103903.
[21] A.A. Frolov, A.V. Borodin, M.N. Esaulkov, A.P. Shkurinov, JETP 141 (2012) 1027.
[22] M.M. Nazarov, A.P. Shkurinov, E.A. Kuleshov, V.V. Tuchin, Quantum Electron. 38 (7) (2008) 647.
[23] B. Delley, J. Chem. Phys. 92 (1990) 508.
[24] B. Delley, J. Chem. Phys. 113 (2000) 7756.
[25] J.P. Perdew, K. Burke, M. Ernzerhof, Phys. Rev. Lett. 77 (1996) 3865.
[26] A. Tkatchenko, M. Scheffler, Phys. Rev. Lett. 102 (2009) 073005.
[27] R. Rudman, R. Lippman, D.S. Sake Gowda, D. Eilerman, Acta Cryst. C 39 (1983) 1267.
[28] E. Maverick, P. Seller, W.B. Schweizer, J.D. Dunitz, Acta Cryst. B 36 (1980) 615.
[29] G.A. Mironova, Moscow MSU 2 (2006) 100.
[30] J.H. Northrop, M. Kunitz and R.M. Herriott. Crystalline enzymes, Columbia Univ. Press, 1948.